Structural Engineering and Mechanics, Vol. 31, No. 5 (2009) 527-544
DOI: http://dx.doi.org/10.12989/sem.2009.31.5.527

Periodic seismic performance evaluation of highway bridges using structural health monitoring system

Jin-Hak Yi†

Coastal Engineering and Ocean Energy Research Department, Korea Ocean Research and Development Institute, Gyeonggi 426-744, Korea

Dookie Kim‡

Department of Civil and Environmental Engineering, Kunsan National University, Jeonbuk, Korea

Maria Q. Feng‡†

Department of Civil and Environmental Engineering, University of California, Irvine, CA92744, USA

(Received August 18, 2008, Accepted February 23, 2009)

Abstract. In this study, the periodic seismic performance evaluation scheme is proposed using a structural health monitoring system in terms of seismic fragility. An instrumented highway bridge is used to demonstrate the evaluation procedure involving (1) measuring ambient vibration of a bridge under general vehicle loadings, (2) identifying modal parameters from the measured acceleration data by applying output-only modal identification method, (3) updating a preliminary finite element model (obtained from structural design drawings) with the identified modal parameters using real-coded genetic algorithm, (4) analyzing nonlinear response time histories of the structure under earthquake excitations, and finally (5) developing fragility curves represented by a log-normal distribution function using maximum likelihood estimation. It is found that the seismic fragility of a highway bridge can be updated using extracted modal parameters and can also be monitored further by utilizing the instrumented structural health monitoring system.

Keywords: seismic performance evaluation; seismic fragility curve; model updating; genetic algorithm; output-only modal identification.

1. Introduction

As the conventional structural design concept based on the prescriptive code focusing on the structural safety is shifting toward the performance-based design, it becomes increasingly important to monitor and evaluate a long-term structural performance as well as structural integrity such as

† Senior Research Scientist, Corresponding author, E-mail: yijh@kordi.re.kr
‡ E-mail: kim2kie@kunsan.ac.kr
‡† E-mail: mfeng@uci.edu

material degradation and cracks. In the case of seismic performance, the existing structures are apt to be deficient to earthquake events, especially if they were built in the periods when the seismic design code was not fully developed. The seismic performance of an existing structure is generally evaluated considering design drawings and visual inspection data. However this approach has a limitation that the degraded material properties such as changes in mass, stiffness and damping ratio cannot be quantitatively considered. These structural changes can be rationally estimated by using structural identification methods reflecting the real structural responses. The structural identification methods are conventionally applied for experimental modal analysis, damage detection, model validation and so on. Herein the structural identification method is applied to evaluate the structural seismic performance of a bridge and to monitor it periodically.

Considering the classification criterion proposed by Rytter (1996), the structural identification methods can be categorized as Level I for alarming damage existence, Level II for locating damage, Level III for measuring damage severity and Level IV for predicting remaining service life and structural performance. The purpose of this study can be classified under the Level IV structural identification. The recent research related to the Level IV identification is briefly introduced herein. Choi *et al.* (2001) carried out forced vibration tests on a large-scale model for the confinement structure of a nuclear power plant built in Hualien, Taiwan, and they identified the frequency response function of the model structure. The material properties of layered soil media and structural members were estimated using inverse analysis based on the gradient decent method, and an updated FE model with estimated material parameters was used to analyze the seismic response under a real earthquake that occurred nearby Hualien. It was found that the calculated response by the updated FE model was very close to the real measurements (Choi *et al.* 2001). Jaishi *et al.* (2003) applied the ambient vibration test to identify the modal properties of Nyatopol Temple, a historic structure in Nepal, and they evaluated the seismic safety of the structure using an updated FE model (Jaishi *et al.* 2003). Shama *et al.* (2001) applied the ambient vibration tests for North Grand Island Bridge in West New York and the identified modal properties were utilized for validating the FE model (Shama *et al.* 2001). A similar study was carried out by Ren *et al.* (2004). They applied the ambient vibration tests for a continuous girder bridge, Cumberland Bridge, and an updated FE model was utilized for evaluating the seismic safety of critical members and bridge shoes. More recently, there was an interesting collaborative research project named as wide-range non-intrusive devices toward the conservation of historical monuments in the Mediterranean area funded by the European Union. This project was carried out from 2004 to 2007, and the main results were reported through the journal papers. Chrysostomou *et al.* (2008a) carried out ambient vibration tests and modal identification for an ancient aqueduct built in 1747 in Cyprus and they found that there were significant gaps between the natural frequencies obtained from June of 2004 and May of 2007 due to the soil structure interaction effects from seasonal variations of the water-level in a nearby salt-lake. The updated FE model with estimated material properties was utilized to test the effectiveness of the shape memory alloy pre-stressed devices in protecting the structure without spoiling its monumental value (Chrysostomou *et al.* 2008b). Similar approaches were done for the Ajloun mosque minaret, a historical monument in Jordan (Bani-Hani *et al.* 2008), for the Zaouia of Sidi Kassm Djilizi Temple built in the 16th century in Tunisia (El-Borgi *et al.* 2008a, 2008b), and for Qusun built in 1337 and the Al-Sultaniya mirarets built in 1340 in Cairo, Egypt (El-Attar *et al.* 2008).

This paper presents a systematic procedure for the evaluation of structural performances under seismic loadings based on measured vibration data under ambient wind and traffic loadings. This

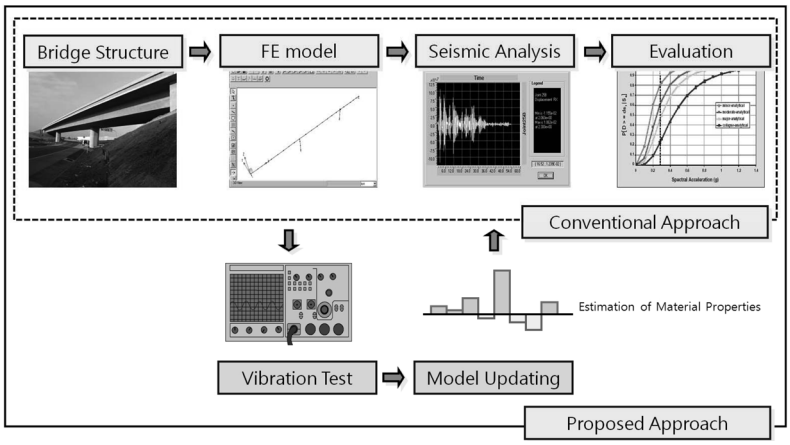

Fig. 1 Schematic diagram of proposed approach to evaluate the seismic performance

proposed procedure includes (1) identification of modal properties based on ambient vibration test using output-only modal identification technique, (2) updating of a preliminary FE model based on identified modal properties by using real-coded genetic algorithm as inverse analysis tool, and (3) evaluation of the structural performance utilizing the updated FE model. Seismic fragility was chosen as the index of seismic performance.

The authors instrumented three highway bridges in Orange County, California, for the evaluation of the structural performance under seismic loads as well as traffic loads. One of the three instrumented bridges, the Jamboree Road Overcrossing, was chosen to demonstrate the full proposed procedure. A preliminary FE model was constructed based on the bridge design drawings and then the FE model was updated based on modal parameters obtained from the measured vibration data. Finally, the structural seismic fragility curves were developed based on both the preliminary FE analysis model and the updated FE model. Fig. 1 shows the schematic diagram of the conventional and proposed seismic performance evaluation procedures.

2. Theoretical backgrounds

2.1 Output-only modal parameter identification

There are several modal identification techniques using output-only information. The most general method in the engineering field might be the power spectral method in which the modal parameters can be identified by reading the peak frequencies and the amplitude of the power spectral density functions (Bendat and Piersol 1993). Recently, the enhanced frequency domain decomposition (EFDD) method was developed using the singular value decomposition of the power spectral density function matrix (Brinker *et al.* 2001). The eigensystem realization algorithm (Juang 1994) and the stochastic subspace identification method (Overschee and De Moor 1996) are also well-known modal identification methods using time history data. Ren *et al.* (2004) and Yi and Yun (2004) carried out the comparative study on several output-only modal identification methods using several data sets of ambient vibration tests. They concluded that the stochastic subspace identification method is the most consistent and reliable method among the tested identification

methods while it requires a lot of computation time. In this study, the stochastic subspace identification method is utilized for a more reliable modal identification with damping estimation.

The stochastic subspace identification method utilizes the singular value decomposition of a block Hankel matrix with a cross correlation matrix of responses. The fundamental basis is the stochastic state space equation, which considers the system dynamics under the stochastic random excitation as

$$\begin{aligned} \mathbf{z}(k+1) &= \mathbf{A}\mathbf{z}(k)+\mathbf{w}(k) \\ \mathbf{y}(k) &= \mathbf{C}\mathbf{z}(k)+\mathbf{v}(k) \end{aligned} \tag{1}$$

where $\mathbf{w}(k)$ and $\mathbf{v}(k)$ are statistically uncorrelated Gaussian random vector sequences with zero means representing the process and measurement noises, respectively. Then, the cross correlation function $\mathbf{R}(k)$ can be calculated as (2)

$$\mathbf{R}(k) = E[\mathbf{y}(k+m)\mathbf{y}(m)^T] = \mathbf{C}\mathbf{A}^{k-1}E[\mathbf{z}(m+1)\mathbf{y}(m)^T] = \mathbf{C}\mathbf{A}^{k-1}\mathbf{G} \tag{2}$$

where $\mathbf{G} \triangleq E[\mathbf{z}(m+1)\mathbf{y}(m)^T]$. Constructing the block Hankel matrix with the cross correlation matrix $\mathbf{R}(k)$, this block Hankel matrix ($\mathbf{H}_{n_1,n_2}$) can be decomposed into an observability matrix ($\mathcal{O}_{n_1}$) and an extended controllability matrix ($\mathcal{C}_{n_2}^{ext}$) as

$$\mathbf{H}_{n_1,n_2} = \begin{bmatrix} \mathbf{R}_1 & \cdots & \mathbf{R}_{n_2} \\ \vdots & \ddots & \vdots \\ \mathbf{R}_{n_1} & \cdots & \mathbf{R}_{n_1+n_2-1} \end{bmatrix} = \begin{bmatrix} \mathbf{CG} & \cdots & \mathbf{CA}^{n_2-1}\mathbf{G} \\ \vdots & \ddots & \vdots \\ \mathbf{CA}^{n_1-1}\mathbf{G} & \cdots & \mathbf{CA}^{n_1+n_2-2}\mathbf{G} \end{bmatrix} = \begin{bmatrix} \mathbf{C} \\ \vdots \\ \mathbf{CA}^{n_1-1} \end{bmatrix} \begin{bmatrix} \mathbf{G} & \cdots & \mathbf{A}^{n_2-1}\mathbf{G} \end{bmatrix} = \mathcal{O}_{n_1}\mathcal{C}_{n_2}^{ext} \tag{3}$$

where $\mathcal{O}_{n_1} \triangleq \left[\mathbf{C}^T \ldots (\mathbf{CA}^{n_1-1})^T\right]^T$, and $\mathcal{C}_{n_2}^{ext} \triangleq \left[\mathbf{G} \ldots \mathbf{A}^{n_2-1}\mathbf{G}\right]$, and n_1 and n_2 are the numbers of the cross-correlation matrix in rows and columns in the block Hankel matrix. Then, the system matrix $\mathbf{A}$ can be obtained using the upper (n_1-1) block matrix deleting the last block row of $\mathcal{O}_{n_1}$ and the lower (n_1-1) block matrix of the upper-shifted matrix by one block row as

$$\mathcal{O}_{n_1-1}^{\uparrow} = \mathcal{O}_{n_1-1}\mathbf{A} \tag{4}$$

where $\mathcal{O}_{n_1-1}^{\uparrow} \triangleq \left[(\mathbf{CA})^T \ldots (\mathbf{CA}^{n_1-1})^T\right]^T$, $\mathcal{O}_{n_1-1} \triangleq \left[\mathbf{C}^T \ldots (\mathbf{CA}^{n_1-2})^T\right]^T$. The eigenvalues and vectors of the discrete system can be calculated from the eigenvalue decomposition of the system matrix $\mathbf{A}$ as follows

$$\mathbf{A}\Psi = \Psi\mathbf{M} \ (\mathbf{M} = diag(\mu_1, \ldots, \mu_N) \in \mathbf{R}^{N\times N} \text{ and } \Psi = [\psi_1, \ldots, \psi_N] \in \mathbf{R}^{N\times N}) \tag{5}$$

Finally, the eigenvalue, modal damping ratio, natural frequency and modal vector for the physical system can be obtained as follows

$$\begin{aligned} \lambda_k &= \frac{1}{\Delta t}\ln\mu_k \\ \xi_k &= -\mathrm{Re}(\lambda_k)/|\lambda_k| \\ \omega_k &= -\mathrm{Im}(\lambda_k)/\sqrt{1-\xi_k^2} \\ \varphi_k &= \mathbf{C}\psi_k \end{aligned} \tag{6}$$

2.2 Updating the numerical FE model using real-coded genetic algorithm

The genetic algorithm (GA) was initiated by observing the mechanism of natural evolution and natural genetics (Holland 1975, Goldberg 1989). It is characterized by a parallel search with multiple solutions called "population" while a point-by-point search is carried out by the conventional optimization methods. An "individual" in the population is a string of symbols called "genes" and each string of genes is referred to as "chromosome" in a binary-coded GA. The chromosome can be converted to a design variable in a physical system. In the case of a real-valued problem, the decimal-coding or grey-coding can be utilized to convert the chromosome into the real design variable. Even though the binary-coded GA has been successfully applied for the real-valued problem (Maity and Tripath 2005, Kim *et al.* 2007), it still has some drawbacks such as a weak local tracking performance near the optimal point. To overcome the limitation of the binary-coded GA for real-valued problems, a real-coded GA was derived to handle the continuous variables efficiently. In the real-coded GA, the concept of a gene disappears and the chromosome is a minimal unit and works as a design variable. The fundamental steps of a real-coded GA are the same as those of a simple binary-coded GA as shown in Fig. 2.

Genetic operations with continuous variables can be carried out in the same way except for the crossover and mutation during reproduction. The crossover and mutation in a real-coded GA were derived by looking into the operation of a binary-coded GA (Kim and Yang 1995). They are explained by the conceptual drawings in Figs. 3 and 4.

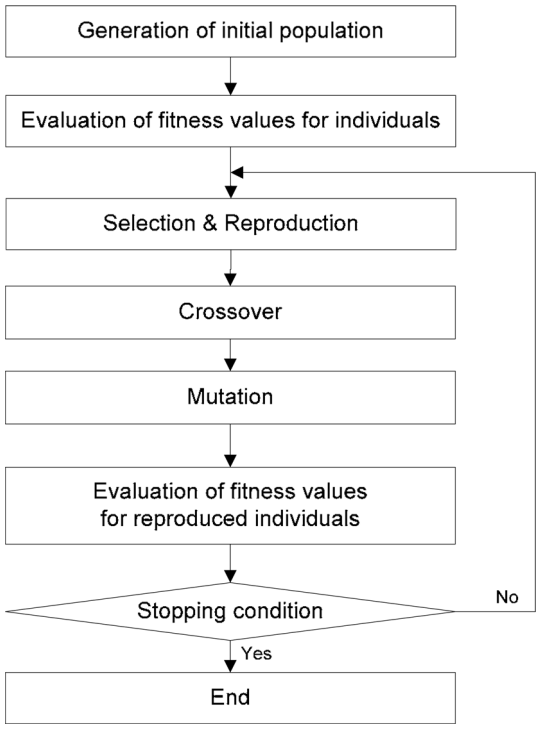

Fig. 2 Basic steps of genetic algorithm

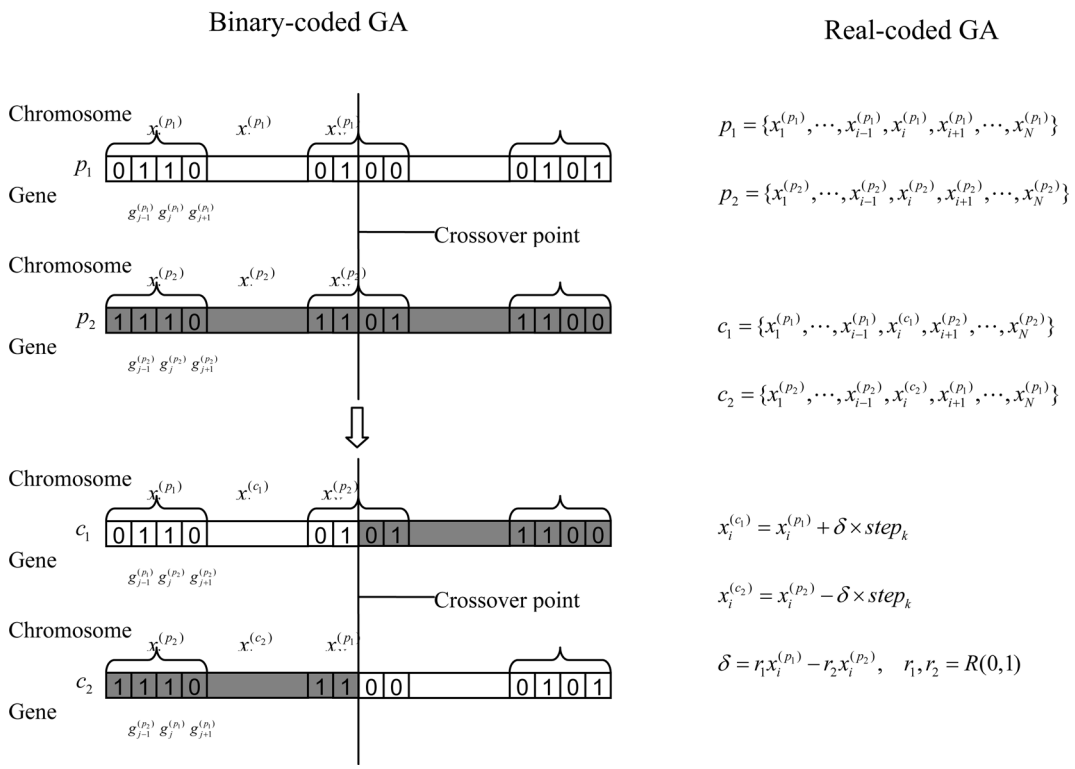

Fig. 3 Comparison of crossover operation between binary- and real-coded GAs

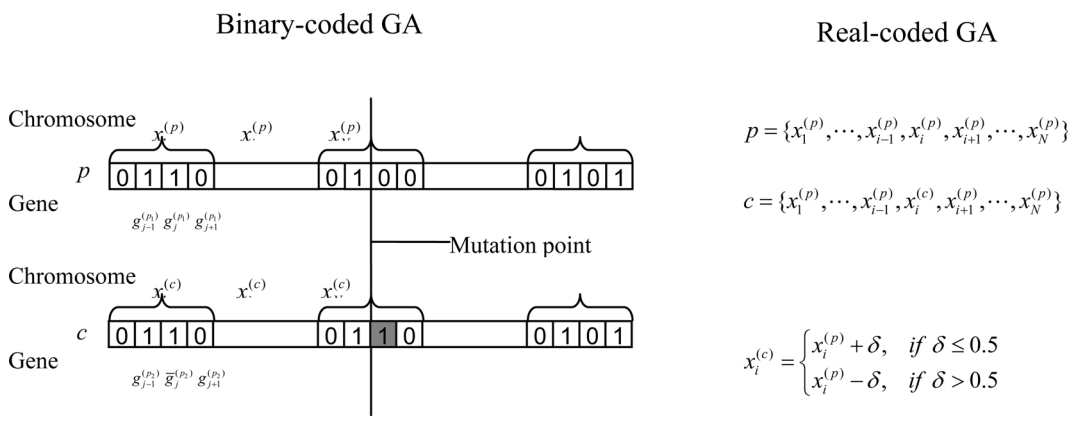

Fig. 4 Comparison of mutation operation between binary- and real-coded GAs

2.3 Seismic performance evaluation using seismic fragility index

In this study, the seismic fragility curves are expressed in the form of a two-parameter log-normal distribution functions as follows. The median (c_k) and the log-standard deviation (ζ_k) of each lognormal distribution are evaluated with the aid of the maximum likelihood estimation. The fragility curve for the k-th damage state $F_k(a)$, takes the following form

$$F_k(a) = \Phi\left[\frac{\ln(a/c_k)}{\zeta_k}\right] \tag{7}$$

where a is a PGA value of the earthquake motion, and $\Phi[\cdot]$ is the standard normal distribution function. The likelihood function for the present purpose can be taken as

$$L = \prod_{i=1}^{N}[F_k(a_i)]^{x_i} \cdot [1 - F_k(a_i)]^{1-x_i}; \tag{8}$$

where x_i is 1 or 0 depending on whether the bridge sustains the k-th damage state under the ground motion with $PGA = a_i$, and N is the number of input ground motion data. Two parameters c_k and ζ_k in Eq. (7) are computed by maximizing the log-likelihood function as

$$\frac{\partial \ln L}{\partial c_k} = \frac{\partial \ln L}{\partial \zeta_k} = 0, \; k = 1, 2, \ldots, N_{state} \tag{9}$$

where N_{state} is the number of damage states considered.

3. Field application

3.1 Description of the test-case bridge

The Jamboree Road Overcrossing, as shown in Fig. 5, is a typical three-span continuous cast-in-place prestressed post-tension box-girder bridge, located in the Eastern Transportation Corridor, Irvine, CA. The total length of the bridge is 110.9 m with span lengths of 35.5, 46.1, and 30.3 m. This bridge is supported on two monolithic single columns and sliding bearings on both abutments. A total of 15 channels of accelerometers are instrumented on the bottom of the bridge girder and a column, as shown in Fig. 5. While the vertical accelerations are usually measured when the structural safety under traffic loads is critical, the transverse accelerations are measured at 5 points on the superstructure since this monitoring system is designed for seismic performance monitoring (Feng *et al.* 2004).

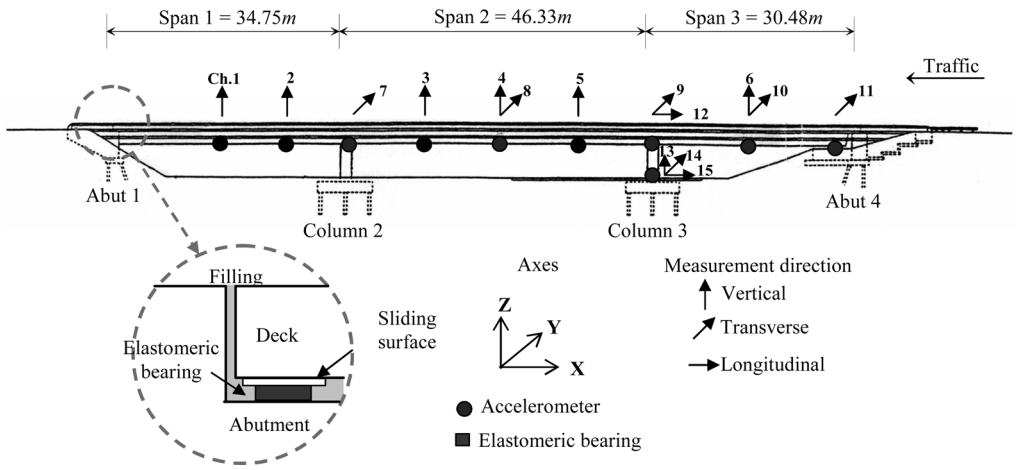

Fig. 5 Description of Jamboree Road Overcrossing

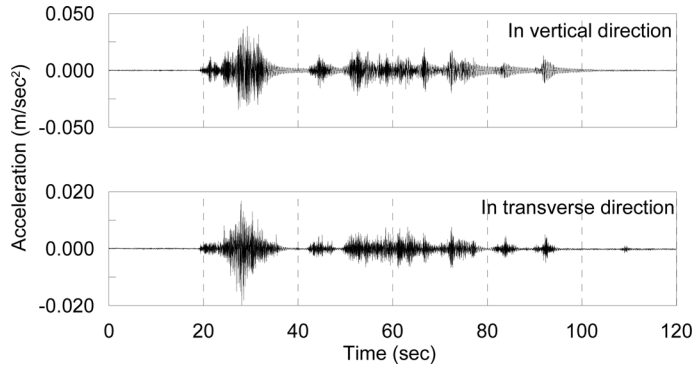

Fig. 6 Typical accelerations in the middle of span 2

Table 1 Estimated modal properties

Modes	Vertical modes		Transverse modes	
	Natural Frequency (Hz)	Modal Damping Ratio (%)	Natural Frequency (Hz)	Modal Damping Ratio (%)
1	2.956 (0.28)	0.79 (18.5)	2.665 (2.60)	2.52 (21.4)
2	4.589 (2.08)	2.82 (16.6)	4.656 (4.80)	2.83 (24.1)
3	6.406 (3.90)	1.62 (58.4)		
4	8.695 (3.76)	3.15 (45.3)		

Note: The values in the parentheses are the coefficients of variation (in %).

3.2 Estimation of modal properties using ambient vibration tests

Ambient vibrations were measured on the Jamboree Road Overcrossing. Accelerations, mainly induced by traffic loads, were measured by the in-structure accelerometers with a sampling frequency of 100 Hz. Typical time histories of accelerations measured at the middle of span 2 in the vertical and transverse directions are shown in Fig. 6. Totally, 82 data sets measured in the daytime were processed, in which the time length of each data set is 10 minutes. As shown in Fig. 6, the vertical acceleration level is higher than the level of transverse acceleration. If the sensor's specifications such as resolution and noise level are the same, the signal to noise ratio for the vertical acceleration is better than that of the transverse one. Hence the modal properties for the vertical modes are expected to be extracted with higher confidence and accuracy.

The stochastic subspace identification method was utilized to extract modal parameters (Peeters and De Roeck 1999) from the measured acceleration data. Table 1 lists the extracted natural frequencies and damping ratios of four lower modes in the vertical direction and of two lower modes in the transverse direction using 82 data sets (measuring time is totally 820 minutes). The values in the parentheses indicate the coefficients of variation (COV) for 82 sets of extracted ones in percent as follows.

$$\mathrm{COV}_{f_j} = \frac{\sigma_{f_i}}{\mu_{f_i}} \times 100(\%), \quad \mathrm{COV}_{\zeta_j} = \frac{\sigma_{\zeta_i}}{\mu_{\zeta_i}} \times 100(\%) \tag{10}$$

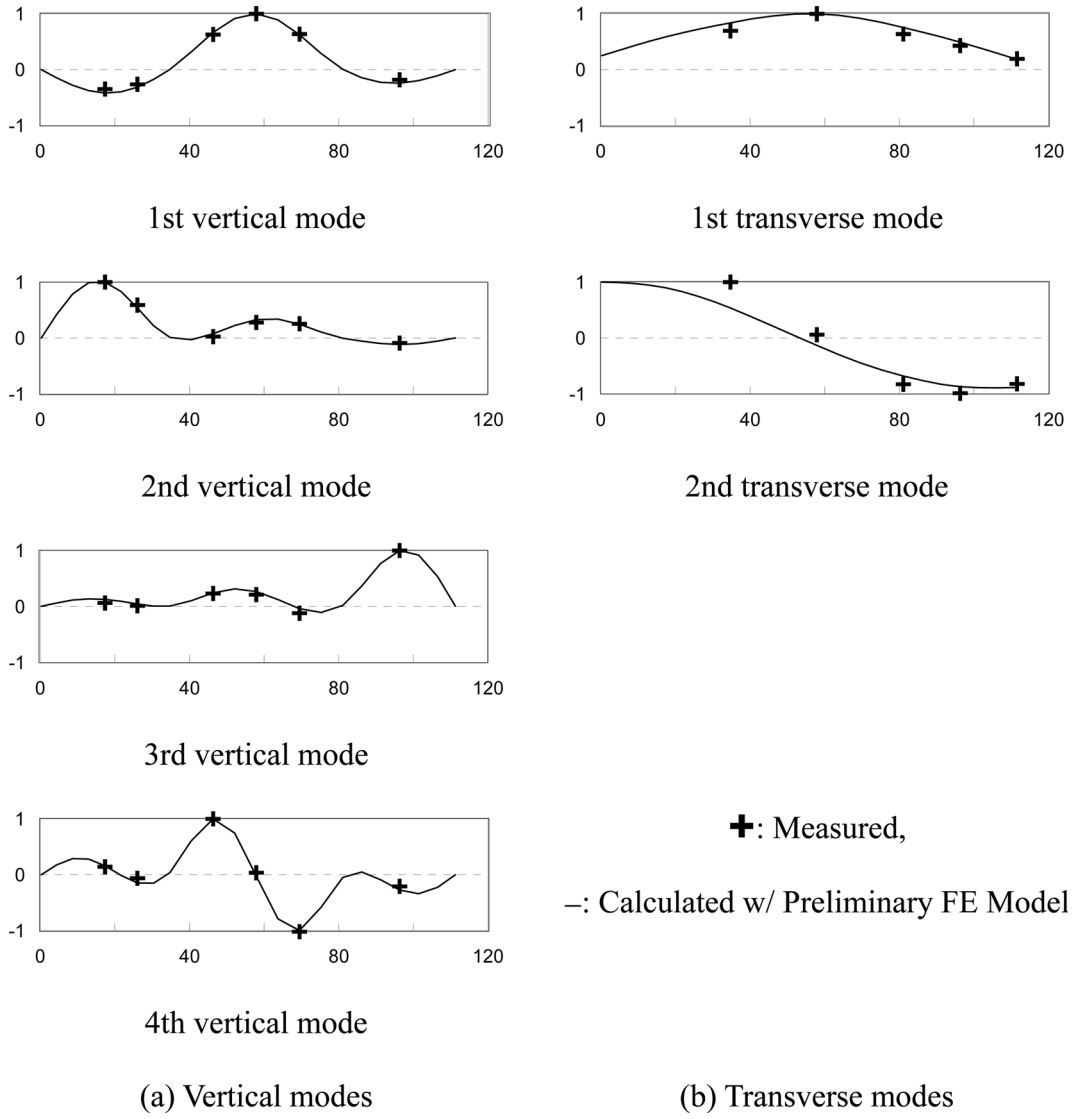

Fig. 7 Comparison of identified mode shapes

where μ and σ are the mean and standard deviation of 82 sets of identified modal parameters, respectively. The COVs for the vertical modes are in the range of 0.28-3.9% while those for the transverse modes are 2.6-4.8%, implying that the estimated natural frequencies for vertical modes are more reliable than those for the transverse modes. This is because traffic loads mainly excite vertical vibrations. Fig. 7 shows mode shapes corresponding to the natural frequencies. It can be also observed that the COVs of the natural frequencies and damping ratios for lower modes are smaller than those of higher modes. This implies that the lower modes are estimated more precisely with higher consistency. The modal damping ratios are estimated at about 0.79-3.15% and these values are relatively lower than the generally accepted modal damping ratio of concrete structures of about 5%. Therefore, it can be said that this bridge is maintained very well based on the fact that

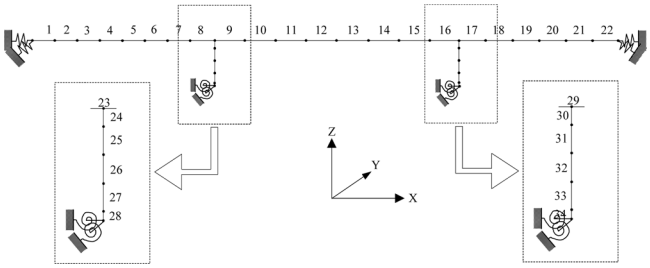

Fig. 8 FE model of a bridge

Table 2 Structural parameters in preliminary FE model

Element	Area (m^2)	Moments of inertia (m^4)		
		Ix	Iy	Iz
Deck	5.94	7.63	3.01	59.36
Column	3.53	2.51	0.72	1.51

the damping ratio is usually increased by structural damages (Liang and Lee 1991, Huang *et al.* 1996).

3.3 Model updating using genetic algorithm

3.3.1 Preliminary FE model and analysis

A 3-D preliminary FE model, as shown in Fig. 8, was developed for the Jamboree Road Overcrossing. The super- and sub-structures were modeled as 3-D frame elements using SAP2000. The cross-sectional area and moment of inertia for each element were calculated from the design drawings and they are listed in Table 2. The supports were modeled as linear and rotational springs with the stiffness values of 1.46×10^7 kN/m and 4.45×10^{10} kN·m/rad, respectively (FHWA 1996), although they are usually assumed as hinged or fixed. The natural frequencies and the mode shapes computed using this numerical model are shown in the third row of Table 5 and the continuous line in Fig. 7. The differences between the numerical and experimental natural frequencies, as shown in the parentheses in Table 5, suggest the need for updating the preliminary FE model using the measured vibration data.

3.3.2 Genetic algorithm-based system identification

The real-coded genetic algorithm (Kim and Yang 1995) was employed for updating the preliminary FE model based on the measured modal properties of the bridge. The objective function represents the differences between the measured and calculated natural frequencies, and the constraint equations were constructed based on the differences between the measured and calculated mode shapes as shown in Eq. (11).

$$J = \sum_{i=1}^{N_m} \left\{ w_i \left(\frac{f_i^c - f_i^m}{f_i^m} \right) \right\}^2 \quad \text{subjected to } \left| \phi_{ji}^c - \phi_{ji}^m \right| \le \varepsilon \tag{11}$$

Table 3 Details of genetic algorithm and weighting factors

Description	Values	Modes	Weighting factor
Number of Individuals	20	Vertical 1st mode	100%
Number of Generations	100	Vertical 2nd mode	50%
Reproduction Method	Proportional	Vertical 3rd mode	25%
Crossover Probability	0.4	Vertical 4th mode	12%
Mutation Probability	0.01	Transverse 1st mode	25%
Elite	10% of Population	Transverse 2nd mode	12%

Table 4 Structural correction coefficients estimated by genetic algorithm

c_1	c_2	c_3	c_4	c_5	c_6	c_7	c_8
0.947	0.957	0.971	1.084	1.082	0.938	1.700	0.269

Table 5 Comparisons of measured and recalculated natural frequencies (Hz)

Modes	Vertical modes				Transverse modes	
	1	2	3	4	1	2
Measured	2.956	4.589	6.406	8.695	2.665	4.656
Preliminary FE model	2.888 (2.30)	4.619 (1.65)	5.726 (10.61)	9.407 (8.19)	3.165 (18.76)	4.199 (9.82)
Updated FE model	2.947 (0.30)	4.662 (1.59)	5.807 (9.35)	9.538 (9.70)	2.675 (0.38)	4.742 (1.85)

Notes: The values in the parentheses are difference (%) between the calculated and measured natural frequencies.

where f_i is the i-th natural frequency, ϕ_{ji} denotes the j-th component of the i-th mode shape $\boldsymbol{\varphi}_i$ which is normalized as $\boldsymbol{\varphi}_i^T \boldsymbol{\varphi}_i = 1$. w_i and ε are the weighting factor for i-th mode and the admissible error bound for the mode shape, respectively. The superscripts "m" and "c" indicate the measured and the calculated data, respectively. Eight structural parameters were used to correlate the FE model with the measured data. There are two sectional areas ($c_1 A^{deck}, c_2 A^{column}$), four moments of inertia ($c_3 I_Y^{deck}, c_4 I_Y^{column}, c_5 I_Z^{deck}, c_6 I_X^{column}$) and one linear spring constant for the abutments ($c_7 k_l^{abutment}$) and one rotational spring constant for the footings ($c_8 k_r^{footing}$), where c_i's are the correction coefficients of the structural parameters. The details for the real-coded genetic algorithm are as shown in Table 3.

The structural correction coefficients estimated by the real-coded genetic algorithm are shown in Table 4. Table 5 compares the modal parameters computed by the updated model with those obtained from the measured vibration data. It is obvious that the natural frequencies of the updated model better agree with the measured ones than those of the preliminary FE model especially for the transverse modes. The differences between the identified and the calculated natural frequencies are not so significantly reduced by updating in the case of vertical modes, i.e. 0.6-10.6% for the preliminary FE model and 0.3-9.7% for the updated FE model. Only the 1st natural frequency is obviously enhanced from 2.3% to 0.3%. In the case of transverse modes, the effectiveness of model

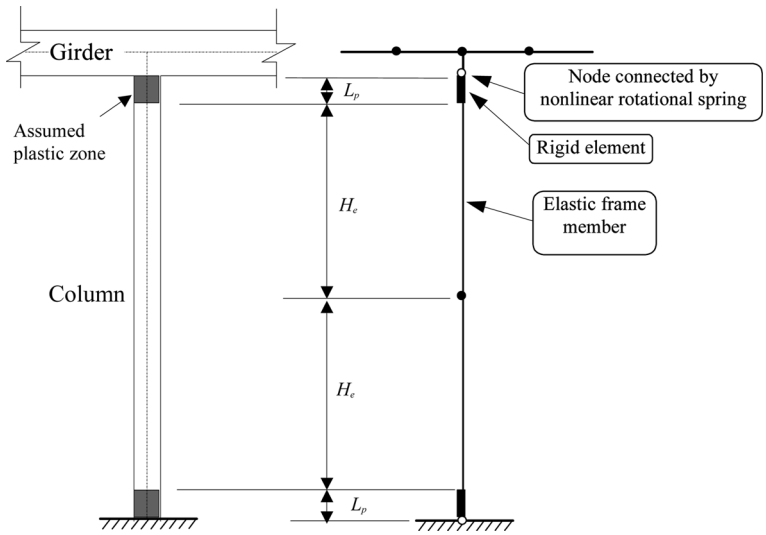

Fig. 9 Modeling of column with plastic hinges

updating is very clear. From Table 5, it can be observed that the differences are significantly reduced from 9.8-18.8% to 0.3-1.9% for the transverse modes. Since the seismic performance of a bridge is generally more related to the transverse vibration characteristics, this result is a quite impressive in the view point of seismic performance evaluation.

As mentioned previously, the vertical vibration modes are not so significantly enhanced by updating, in other word, this implies that the preliminary FE model has a relatively good performance to analyze vertical vibration responses. Considering the vibration modeshapes in Fig. 7, it can be found that the properties of a bridge deck significantly affect the vertical modes while the properties of all sub-systems including the bridge deck, column, abutment and foundation affect more the transverse vibration modes. And it reveals that the bridge deck of the preliminary FE model is already accurately modeled while the abutment and foundation are not so reliably modeled, and the effects of abutment and foundation are reasonably updated by adjusting the spring constants for abutment and foundation using measured modal data.

3.4 Seismic fragility analysis

Seismic fragility analysis was performed on the Jamboree Road Overcrossing. In developing the seismic fragility curves, nonlinear response time histories were analyzed using the computer code SAP2000 under the sixty (60) Los Angeles earthquake time histories selected for the FEMA SAC project (SAC Joint Venture 1997). Both the preliminary and the updated FE models were used. The parameter used to describe the nonlinear structural response in this study is the ductility demand. The ductility demand is defined as θ/θ_y, where θ is the rotation of a bridge column in its plastic hinge and θ_y is the corresponding rotation at the yield point.

3.4.1 Nonlinear modeling and seismic response analysis

Both of the preliminary FE model and the updated FE model of the Jamboree Road Overcrossing presented earlier are linear models. However, intensive earthquake will cause the

bridge columns to yield. In order to study seismic fragility based on seismic time history analysis, a nonlinear bridge model must be developed. For the purpose of this study, the bridge column is modeled as an elastic zone with a pair of plastic zones at each end of the column considering a double bending behavior.

Nonlinear responses of the bridge are simulated based on analysis of the moment-rotation relationships of the concrete columns with axial loads as well as confinement effects taken into account. The moment-rotation relationship was modeled as bilinear without stiffness degradation. Its parameters were established using a computer code developed by Kushiyama (2002).

Moment-rotation curves obtained using the structural parameters of the preliminary and updated FE models are plotted in Fig. 10 and the parameters are in Table 6. We can observe that the two curves are quite similar. This is partially because the structural parameters updated based on the ambient vibration data are for a linear structural model. The nonlinear parameters were assumed to be the same for both models, which were based on reinforcing steels.

Five (5) different damage states are introduced following the Dutta and Mander (2002)

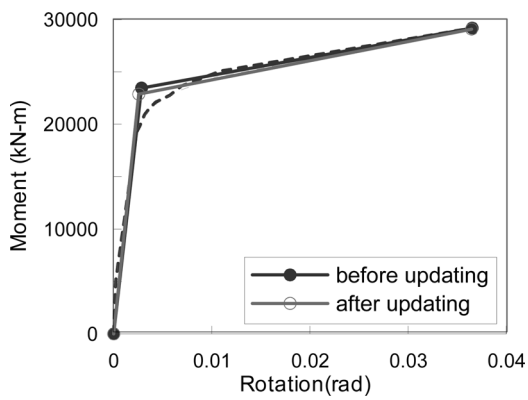

Fig. 10 Moment-rotation curves for Jamboree Road Overcrossing

Table 6 Plastic hinge properties

	θ_y (rad)	θ_u (rad)	k_{eff} ($\times 10^6$ kN-m)	α
Preliminary FE model	0.0028	0.0365	8.281	0.0205
Updated FE model	0.0026	0.0365	8.965	0.0204

Table 7 Description of damage states

Damage state	Description	Drift limits	Rotational ductility limits	
			Preliminary	Updated
Almost no	First yield	0.005	1.00	1.00
Slight	Cracking, spalling	0.007	1.23	1.23
Moderate	Loss of anchorage	0.015	2.19	2.18
Extensive	Incipient column collapse	0.025	3.38	3.37
Complete	Column collapse	0.050	6.36	6.33

recommendations. Table 7 displays the description of these five damage states and the corresponding drift limits for a typical column. For each limit state, the drift limit can be transformed to peak ductility demand of the column for the purpose of this study.

Using the nonlinear models, seismic responses of the Jamboree Road Overcrossing under the 60 ground motions were analyzed. Rotations at the bottom and accelerations at the top of Column 2 under San Fernando earthquake (1971), El Centro earthquake (1940) and Northridge earthquake (1994) are plotted in Fig. 11. We can observe that the maximum values of the acceleration responses from the preliminary and the updated FE models are almost same, while the maximum rotational displacements of the updated FE model is reduced to about 50% of that of the preliminary FE model under the El Centro and Northridge earthquakes. Fig. 12 compares the maximum rotational displacement at the bottom of Column 2 under 60 earthquakes. From the

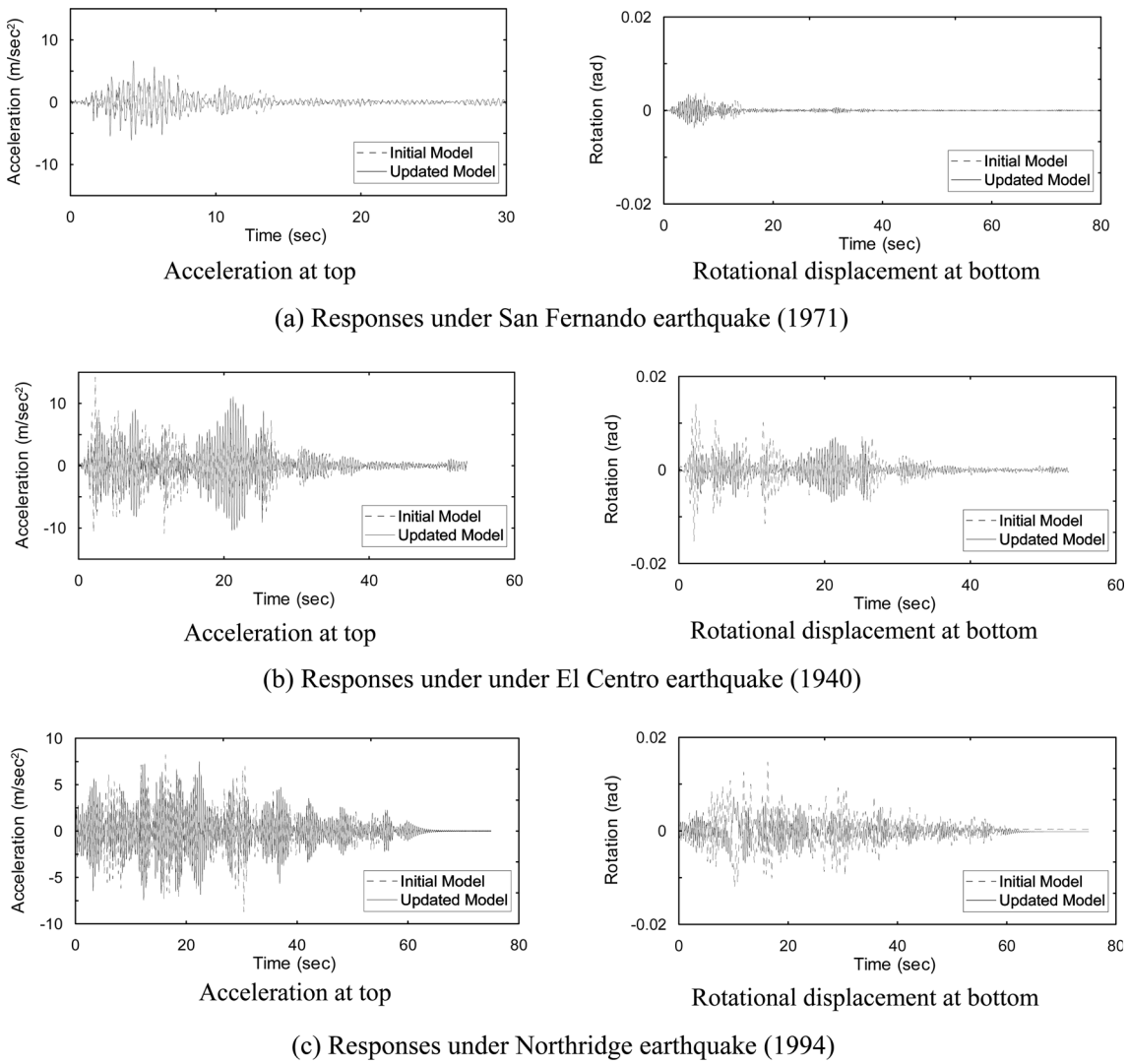

Acceleration at top

Rotational displacement at bottom

(a) Responses under San Fernando earthquake (1971)

Acceleration at top

Rotational displacement at bottom

(b) Responses under under El Centro earthquake (1940)

Acceleration at top

Rotational displacement at bottom

(c) Responses under Northridge earthquake (1994)

Fig. 11 Accelerations and rotational displacements of an example bridge

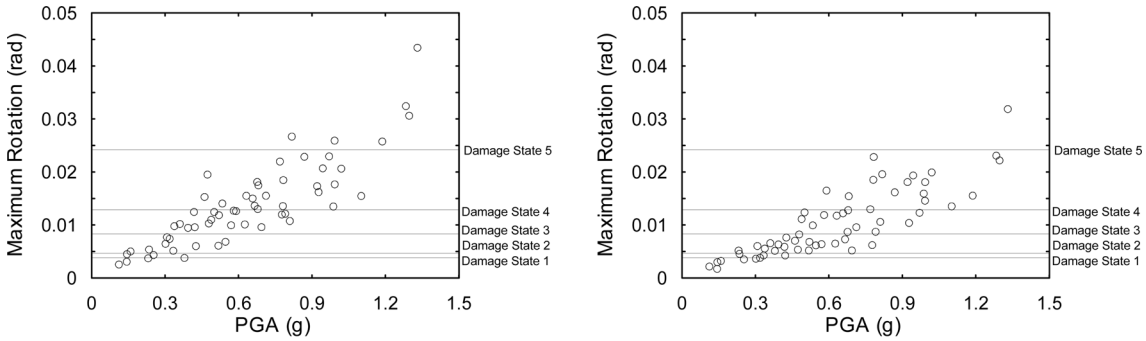

(a) by preliminary FE model (b) by updated FE model

Fig. 12 Maximum rotational displacement at bottom of Column 2

Table 8 Median Values (c_k) and log-standard deviations (ζ_k) of fragility curves

	Before	After	Difference[1)] (%)
Almost no damage	0.159(0.535)[2)]	0.252(0.270)	45.16 (65.8)
Slight	0.215(0.392)	0.302(0.277)	33.53 (34.4)
Moderate	0.386(0.257)	0.583(0.225)	40.67 (13.3)
Extensive	0.621(0.279)	0.808(0.212)	26.12 (27.3)
Complete	1.084(0.168)	1.305(0.201)	18.54 (17.4)

[1)] Difference of a and $b = 2\frac{|a-b|}{a+b} \times 100(\%)$

[2)] The values in the parenthesis are the log-standard deviations.

results, the earthquake responses obtained from the updated FE model are overall reduced, and especially the number of collapse damage reduced from 6 to 1 by adopting the updated FE model. This means that the seismic performance of the bridge is underestimated by using the preliminary FE model.

3.4.2 Fragility curves

The fragility curves for the Jamboree Road Overcrossing are plotted in Fig. 13 as a function of the peak ground acceleration. It is noted that the log-standard deviation for a pair of fragility curves in each plot is obtained by averaging the optimal values from Eq. (10).

It is observed that the fragility for the updated structural model (based on vibration measurement data) is lower than that for the preliminary FE model (based on design drawings). This implies that the Jamboree Road Overcrossing is less vulnerable to seismic damages than what was evaluated utilizing preliminary FE model. It is difficult to find out any trend in the fragility difference as the damage state becomes severe, because the fragility analysis is highly nonlinear and stochastic. The differences of the median values under the longitudinal excitations are in the range of 18-46% in the case of median values and in the range of 17-66% in the case of log-standard deviation values.

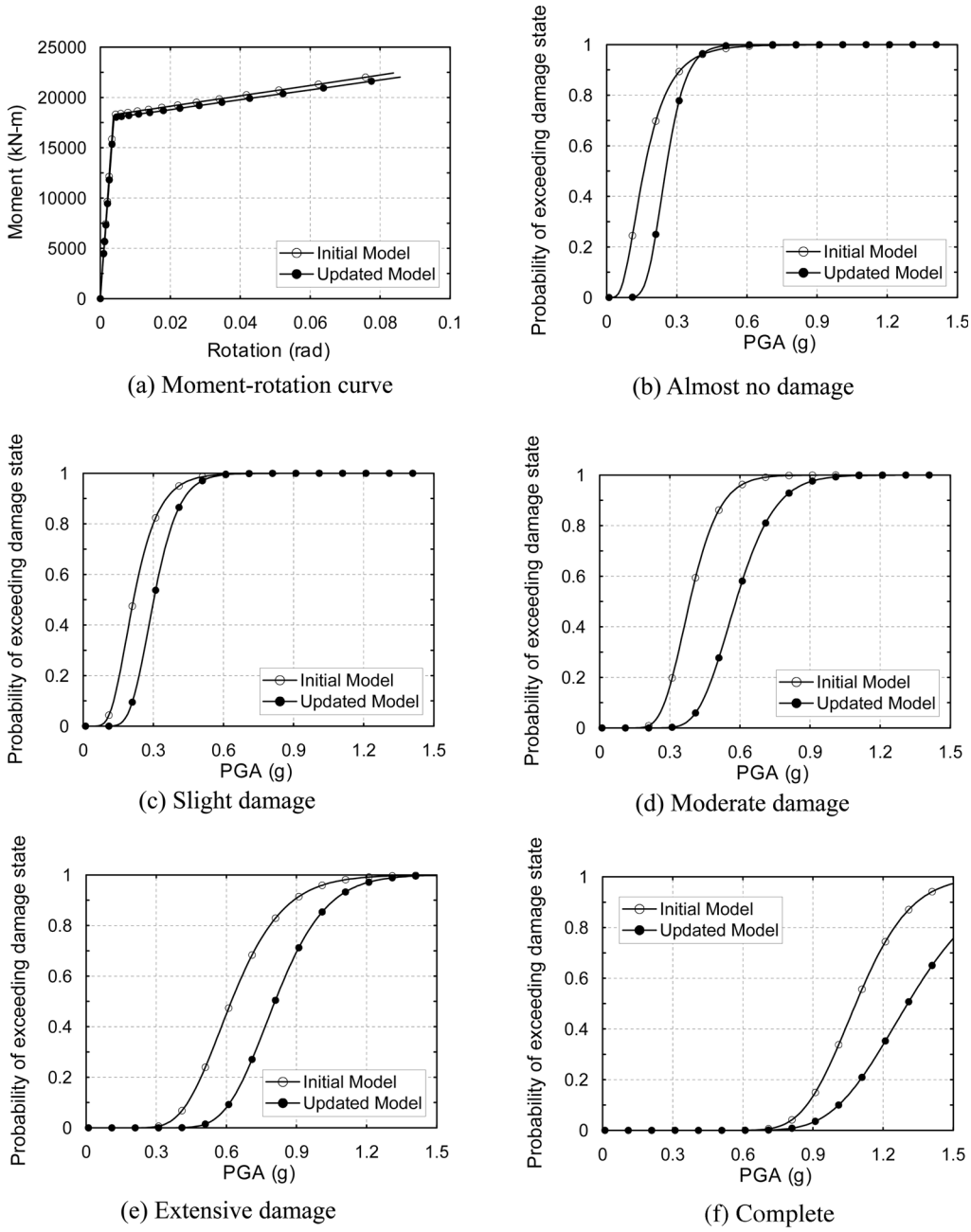

Fig. 13 Fragility curves for Jamboree Road Overcrossing

4. Conclusions

This paper represents the first effort in seismic fragility analysis using a structural analysis model updated with measured ambient vibration data. The following observations and conclusions can be made.

1) The ambient vibration tests were carried out on the instrumented bridge and the modal properties were extracted from the stochastic subspace identification. The vertical modes were more reliably estimated than the transverse modes.

2) The real-coded genetic algorithm was utilized to update the preliminary FE model based on the measured modal data. The transverse modes are significantly enhanced by model updating while the vertical modes are not because the vertical modes are highly affected by deck properties and the bridge deck can be more reasonably modeled than the abutment and footings. After updating, the errors for the natural frequencies were reduced from the range of 9.8-18.8% to the range of 0.3-1.9% in the case of transverse modes, which are generally more related to the seismic performance of a bridge. The abutment and footing properties were substantially adjusted by using measured data.

3) The seismic fragility for the bridge was evaluated utilizing the preliminary FE model and also the updated FE model. Differences were observed between the fragility curves for the preliminary and the updated FE model. The fragility curves can be more reliably evaluated by utilizing the updated model. The modal damping ratios are found to be in the range of 0.7-3.0% while it is known at about 5% in general, and this implies that the bridge is maintained very well by applying the energy dissipation rule, and the same result is conducted from the seismic performance evaluation based on real measurements.

4) By periodically updating the baseline based on the measured vibration data, the structural seismic performance can be periodically evaluated. Even though the linear properties are updated in this study, the nonlinear properties can be updated later, and it is expected that the seismic performance can be more reliably evaluated using updated linear and nonlinear structural parameters.

Acknowledgements

This research was supported by the Ministry of Education, Science and Technology (MEST) and Korea Science and Engineering Foundation (KOSEF) as a part of the Nuclear R&D Program. The bridge instrumentation presented in this study was sponsored by the California Department of Transportation. The authors express their appreciation for the financial support.

References

Bani-Hani, K.A., Zibdeh, H.S. and Hamdaouri, K. (2008), "Health monitoring of a historical monument in Jordan based on ambient vibration test", *Smart Struct. Syst.*, **4**(2), 195-208.

Bendat, J.S. and Piersol, A.G. (1993), Engineering Applications of Correlation and Spectral Analysis, John Wiley & Sons, New York, USA.

Brincker, R., Ventura, C. and Andersen, P. (2001), "Damping estimation by frequency domain decomposition", *Proceedings of the 19th International Modal Analysis Conference*, Kissimee, Florida, 2001.

Chai, Y.H., Priestley, M.J.N. and Seible, F. (1991), "Seismic retrofit of circular bridge columns for enhanced flexural performance", *ACI Struct. J.*, **88**(5), 572-584.

Choi, J.S., Yun C.B. and Kim, J.M. (2001), "Earthquake response analysis of the Hualien soil-structure interaction system based on updated soil properties using forced vibration test data", *Earthq. Eng. Struct. Dyn.*, **30**(1), 1-26.

Chrysostomou, C., Stassis, A. and Demetriou, T. (2008), "Application of shape memory alloy prestressing devices on an ancient aqueduct", *Smart Struct. Syst.*, **4**(2), 261-278.

Chrysostomou, C.Z., Demetriou, T. and Stassis, A. (2008), "Health-monitoring and system-identification of an ancient aqueduct", *Smart Struct. Syst.*, **4**(2), 183-194.

Dutta, A. and Mander, J.B. (2002), "Rapid and detailed seismic fragility analysis of highway bridges", Technical Report at Multidisciplinary Center for Earthquake Engineering, USA.

Ei-Borgi, S., Choura, S., Neifar, M., Smaoui, H., Majdoub, M.S. and Cherif, D. (2008), "Seismic vulnerability assessment of a historical building in Tunisia", *Smart Struct. Syst.*, **4**(2), 209-220.

Ei-Borgi, S., Neifar, M., Ben Jabeur, M., Cherif, D. and Smaoui, H. (2008), "Use of copper shape memory alloys in retrofitting historical monuments", *Smart Struct. Syst.*, **4**(2), 247-260.

El-Attar, A., Saleh, A., El-Habbal, I., Zaghw A.H. and Osman, A. (2008), "The use of SMA wire dampers to enhance the seismic performance of two historical Islamic minarets", *Smart Struct. Syst.*, **4**(2), 221-232.

Feng, M.Q., Kim, D.K., Yi, J.H. and Chen, Y. (2004), "Baseline models for bridge performance monitoring", *J. Eng. Mech.,* ASCE, **130**(5), 562-569.

Goldberg, D.E. (1989), "Genetic algorithms in search, optimization, and machine learning", Addison-Wesley: Reading, MA, USA.

Holland, J.H. (1975), *Adaptation in Natural and Artificial Systems*, University of Michigan, USA.

Huang, J., Liang, Z. and Lee, G.C. (1996), "Structural damage detection using energy transfer ratios (ETR) technique", *Proceedings of the 14th International Modal Analysis Conference*, Dearborn, MI, February 12-15, 1996.

Jaishi, B., Ren, W.-X., Zong, Z.-H. and Maskey, P.N. (2003), "Dynamic and seismic performance of old multi-tiered temples in Nepal", *Eng. Struct.*, **25**(14), 1827-1839.

Juang, J.N. (1994), *Applied System Identification*, Prentice Hall, Englewood Cliffs, New Jersey, USA.

Kim, J.T., Park, J.H., Yoon, H.S. and Yi, J.H. (2007), "Vibration-based damage detection in beams using genetic algorithm", *Smart Struct. Syst.*, **3**(3), 263-280.

Kim, G.H. and Yang, Y.S. (1995), "A real coded genetic algorithm for optimum design", *J. Comput. Struct. Eng. in Korea*, **8**(2).

Kushiyama, S. (2002), Calculation moment-rotation relationship of reinforced concrete member with/without steel jacket, Unpublished Report at University of Southern California, CA, USA.

Liang, Z. and Lee, G.C. (1991), Damping of Structures : Part -Theory of Complex Damping, NCEER Report 91-0004, 1991.

Maity, D. and Tripathy, R.R. (2005), "Damage assessment of structures from changes in natural frequencies using genetic algorithm", *Struct. Eng. Mech.*, **19**(1), 21-42.

Overschee, V.P. and De Moor, B. (1996), Subspace Identification for Linear Systems, Kluwer Academic Publisher.

Peeters, B. and De Roeck, G. (1999), "Reference-based stochastic subspace identification for output-only modal analysis", *Mech. Syst. Signal Pr.*, **13**(6), 855-878.

Priestley, M.J.N., Seible, F. and Calvi, G.M. (1996), Seismic Design and Retrofit of Bridges. John Wiley & Sons, Inc.

Ren, W.X. and Zong, Z.H. (2004), "Output-only modal parameter identification of civil engineering structures", *Struct. Eng. Mech.*, **17**(3-4), 429-444.

Ren, W.X., Zatar, W. and Harik, I.E. (2004), "Ambient vibration-based seismic evaluation of a continuous girder bridge", *Eng. Struct.*, **26**(5) 631-640.

Rytter, A. (1993), Vibration Based Inspection of Civil Engineering Structures, Ph.D. Dissertation, Dept. of Building Technology and Structural Eng., Aalborg University, Denmark.

SAC Joint Venture, Development of Ground Motion Time Histories for Phase 2 of the FEMA/SAC Steel Projects, Report No. SAC/BD-97/04, October 15, 1997.

SAP2000 v.7.44 User Manual. 2002. Computer and Structure, CA, USA.

Shama, A.A., Mander, J.B., Chen, S.S. and Aref, A.J. (2001), "Ambient vibration and seismic evaluation of a cantilever truss bridge", *Eng. Struct.*, **23**, 1281-1292.

Shinozuka, M., Feng. M.Q., Kim, H.-K., Uzawa, T. and Ueda, T. (2002), Statistical analysis of fragility curves, Technical Report at Multidisciplinary Center for Earthquake Engineering, USA.

Yi, J.H. and Yun, C.B. (2004), "Comparative study on modal identification methods using output-only information", *Struct. Eng. Mech.*, **17**(3-4), 445-466.